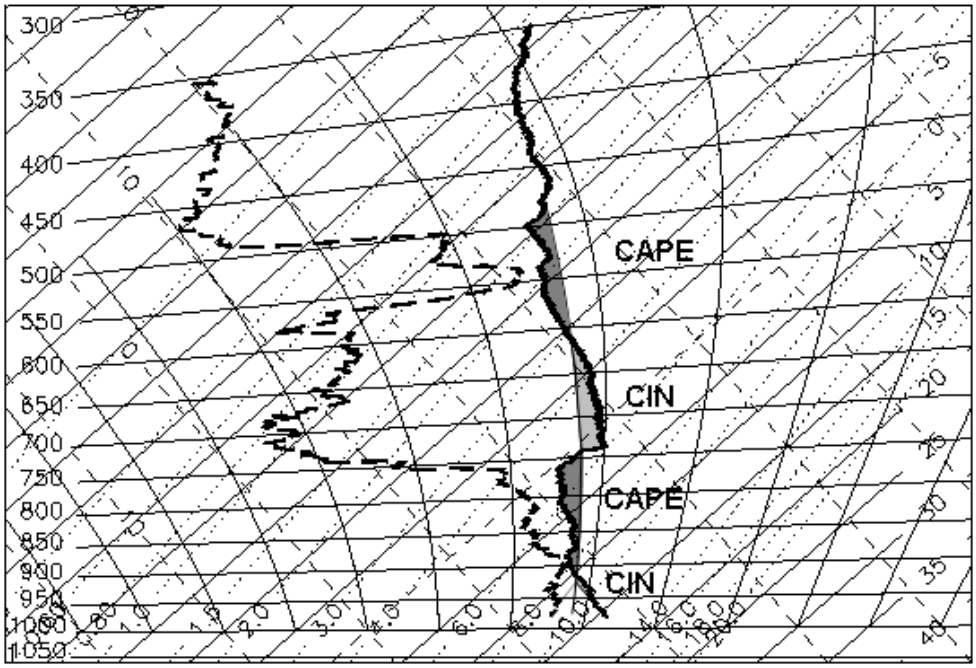

Figure 1: Tephigram for radiosonde launched from Bath at 1100 UTC on 15 June 2005 (IOP 1). The CAPE and CIN are shaded dark and light gray, respectively; the thin solid line partially bounding these areas is the 14C saturated adiabat representing a parcel that ascends unmixed from the boundary layer.

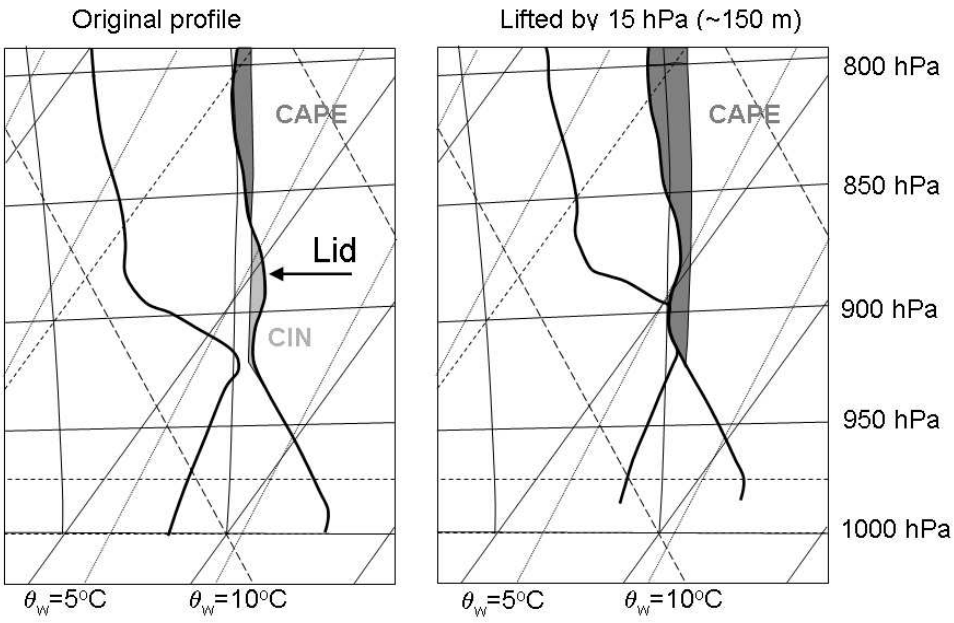

Figure 2: Illustration of how adiabatic lifting of a profile by as little as 15 hPa (about 150 m), can increase the CAPE and completely eliminate the CIN. The original profile is shown on the left and the lifted profile on the right. (Adapted from Morcrette et al. 2006).

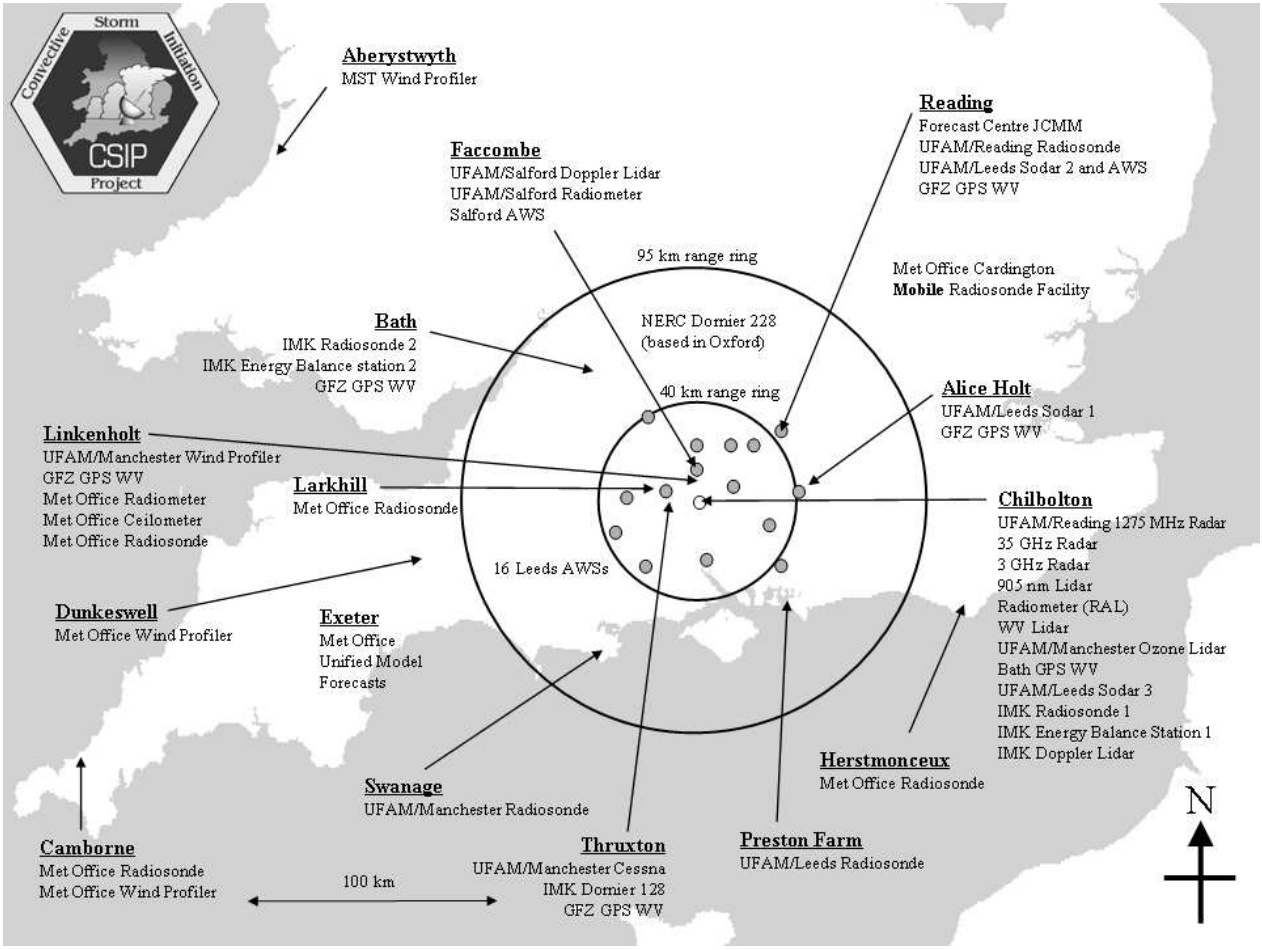

Figure 3: Map showing locations of instruments deployed in southern Britain during CSIP in June, July and August 2005. The shaded circles represent the position of the Automatic Weather Stations (AWSs).

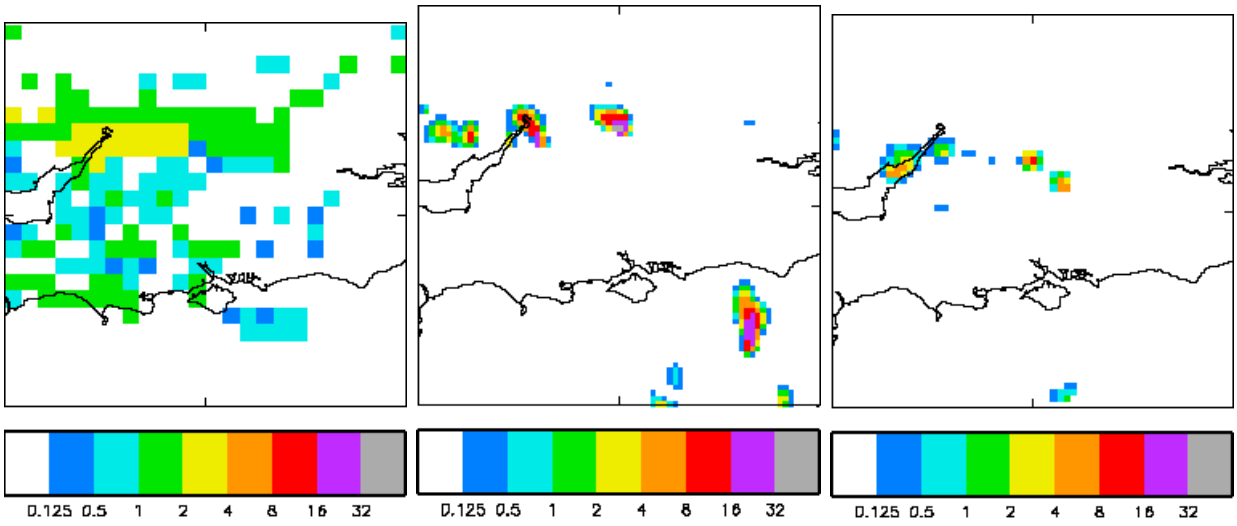

Figure 4: Example of a 13-h precipitation forecast from the Met Office Unified Model run using (from left to right) (a) a 12-km grid and (b) a 4-km grid, compared with (c) the rainfall rate observed by the weather radar network at 1300 UTC on 29 June 2005 (IOP 5). Key gives rainfall intensity in mm h^{-1}.

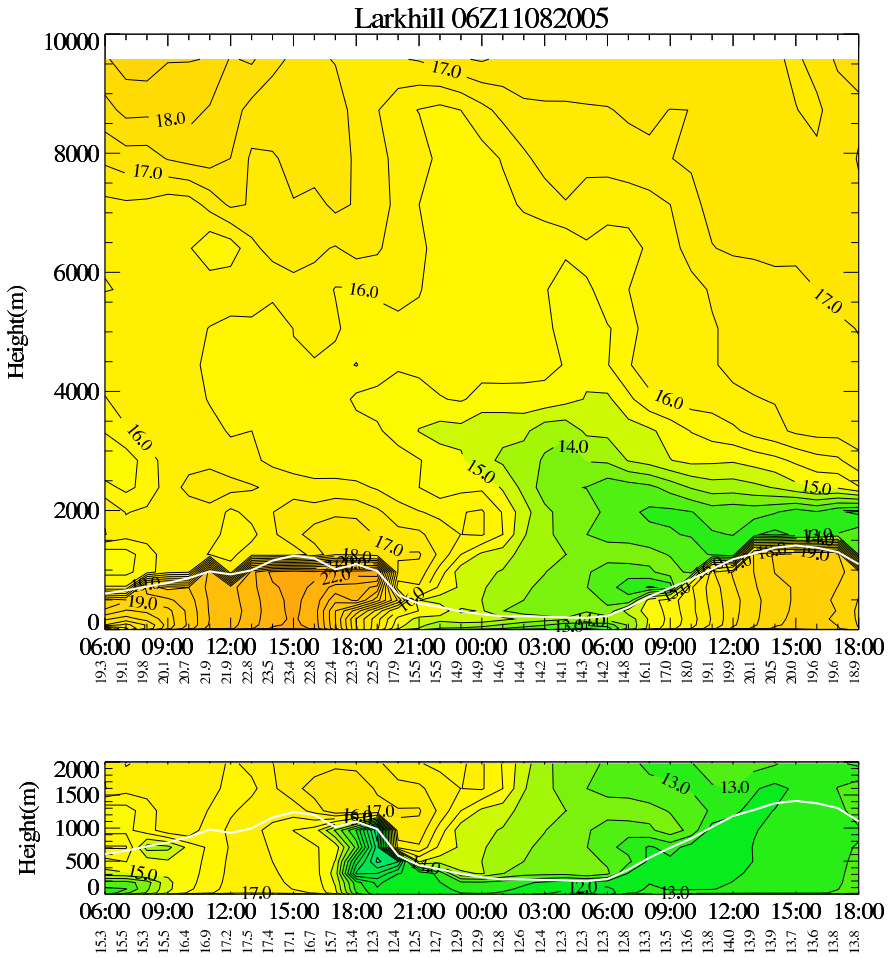

Figure 5: Met Office 12-km-grid Unified Model forecast of the time-height cross-section of θ_s over Larkhill (see Fig. 3 for location) on 11 August (IOP 14R) and 12 August 2005. The white line in the upper plot shows the lifting condensation level; above this the contours and shading represent θ_s and below they represent θ. (Surface values of θ are specified along the time axis of the upper plot). The lower plot shows θ_w.

(a)

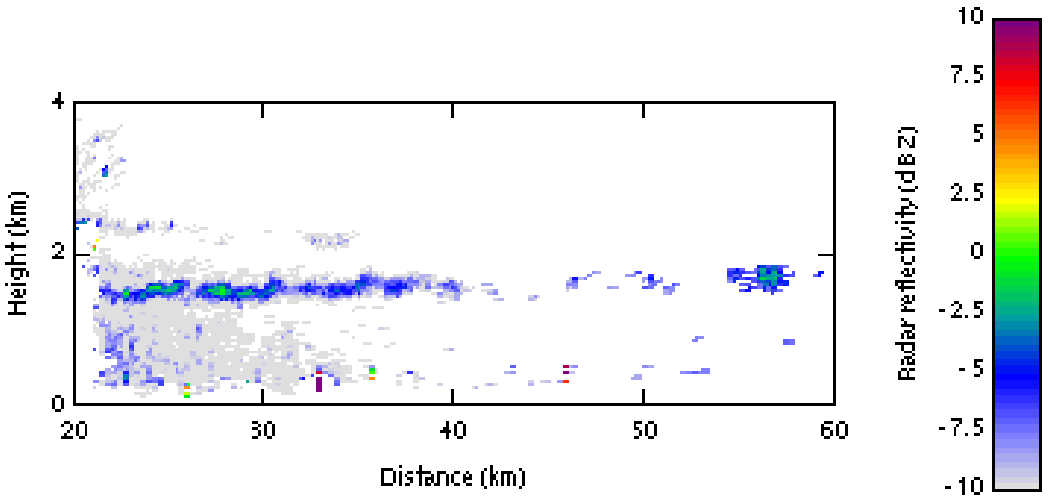

(b)

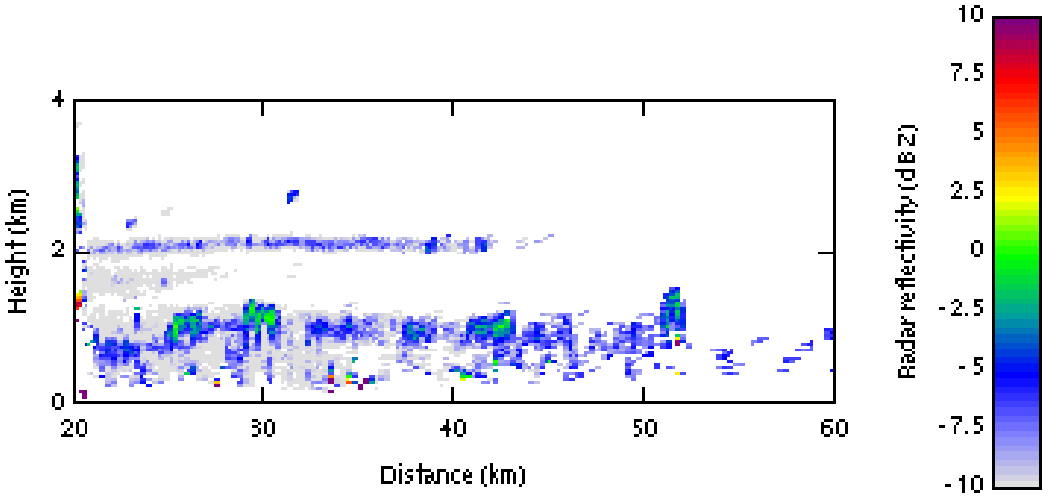

Figure 6: Two examples of RHI scans of reflectivity (dBZ) from the 3 GHz radar at Chilbolton showing lids and the outline of thermals: (a) echo from the bottom of a lid without significant convection beneath it; (b) thermals in the boundary layer below the bottom of a lid (at 1125 UTC on 18 July 2005 (IOP 9) and 1011 UTC on 29 June 2005 (IOP 5), respectively).

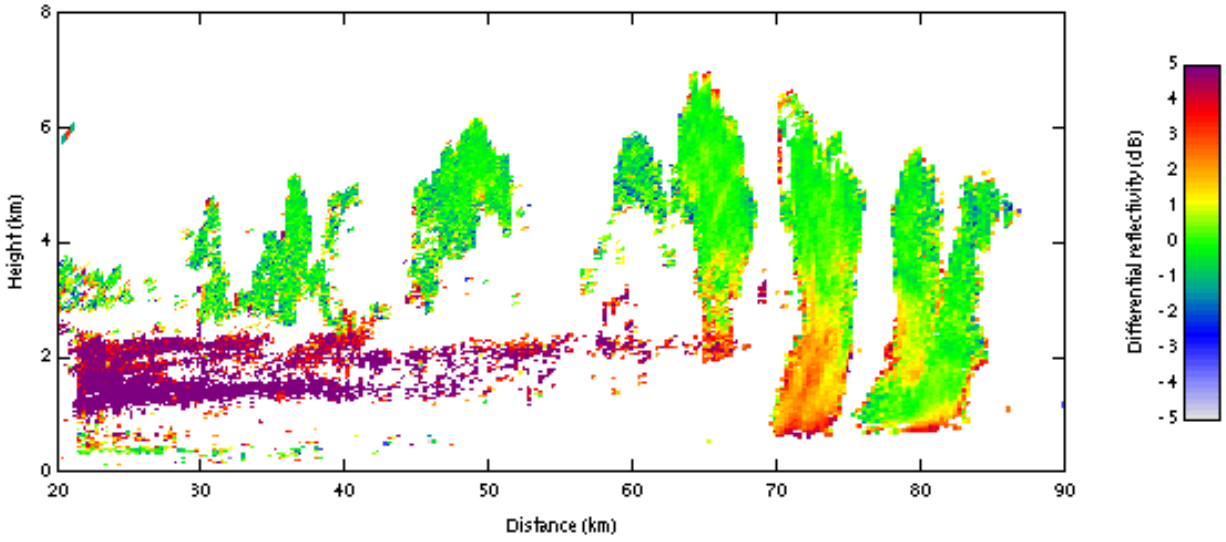

Figure 7: RHI of differential reflectivity (ZDR), from the 3 GHz Chilbolton radar, at 1249 UTC on 24 June 2005 (IOP 3), showing elevated convective cells forming above a stable frontal zone.

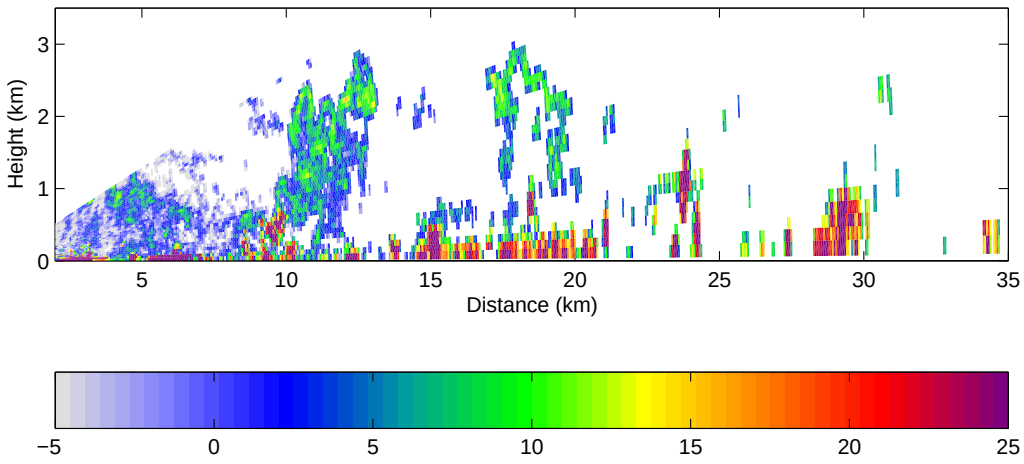

Figure 8: RHI of reflectivity (dBZ) from the 1275 MHz Chilbolton radar at 0928 UTC on 10 July 2004, showing developing cumulus congestus clouds. The echoes near the ground are a combination of ground clutter and returns from insects. (From Morcrette et al. 2006).

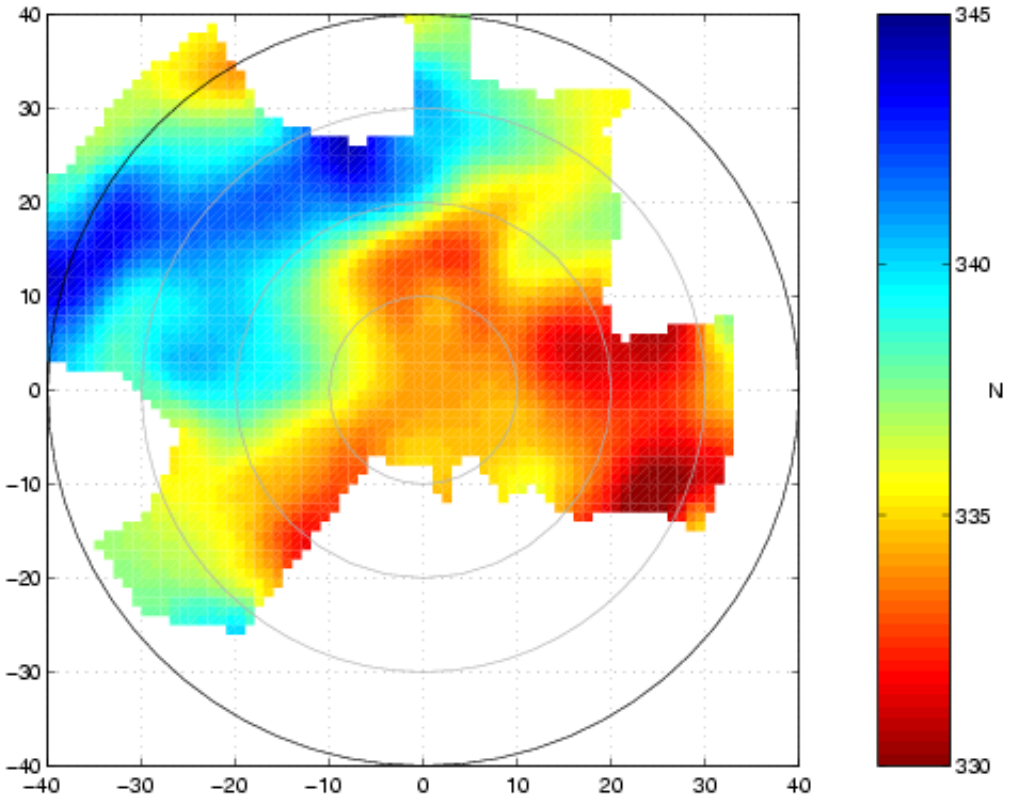

Figure 9: Refractivity field obtained from the 1275 MHz Chilbolton radar at 1259 UTC on 13 July 2005 (IOP 8), using the technique described by Fabry et al. (1997). In summer, the changes in refractivity are mainly due to humidity variations. Here, a change in refractivity of 1 N is approximately equal to a change in relative humidity of 1%.

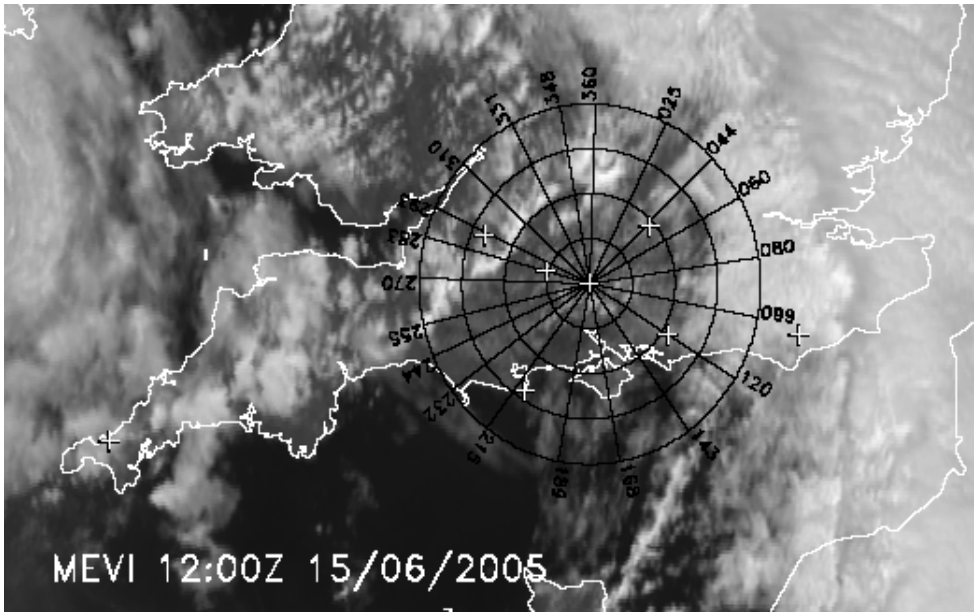

Figure 10: High-resolution visible image from Meteosat-8 (MSG) at 1200 UTC on 15 June 2005 (IOP 1), showing convective cloud along a convergence line extending from the south coast toward the north-east. Range rings are centered on Chilbolton and plotted every 25 km. The radial lines correspond to azimuths with low horizons along which series of RHI scans were obtained.

(a)

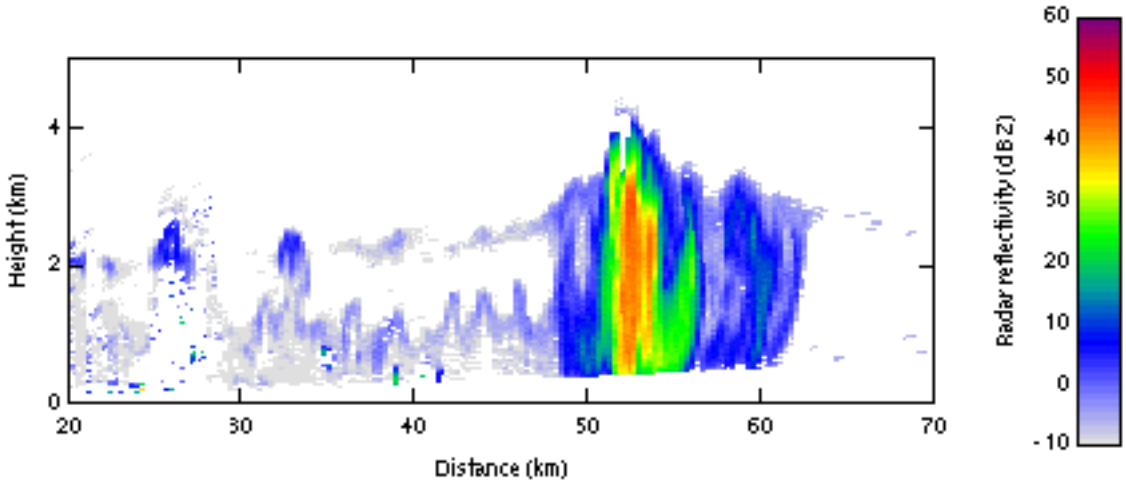

(b)

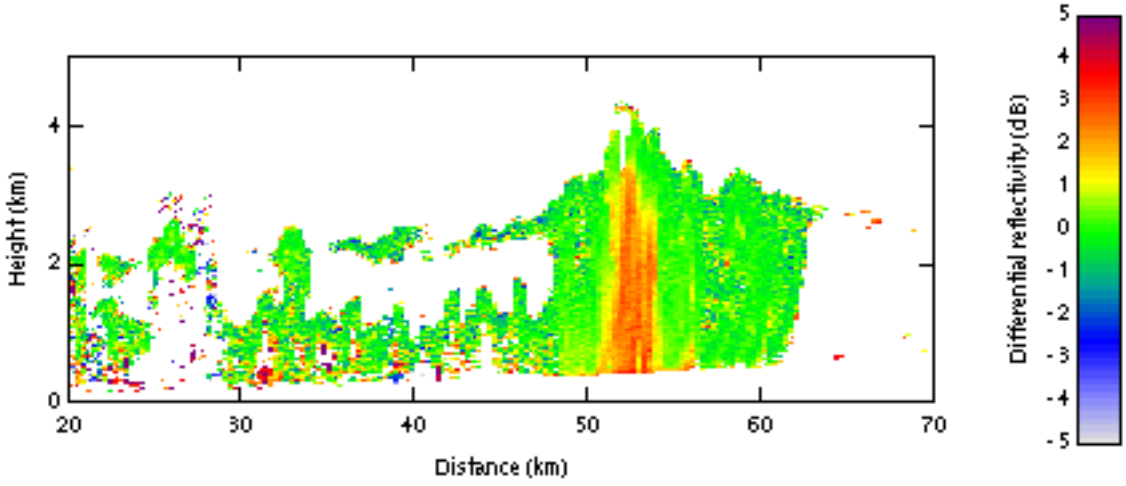

Figure 11: RHIs of (a) reflectivity (dBZ) and (b) differential reflectivity (dB) for a scan across the convergence line shown in Fig. 10, obtained from the 3 GHz Chilbolton radar at 1200 UTC on 15 June 2005 (IOP 1).

(a)

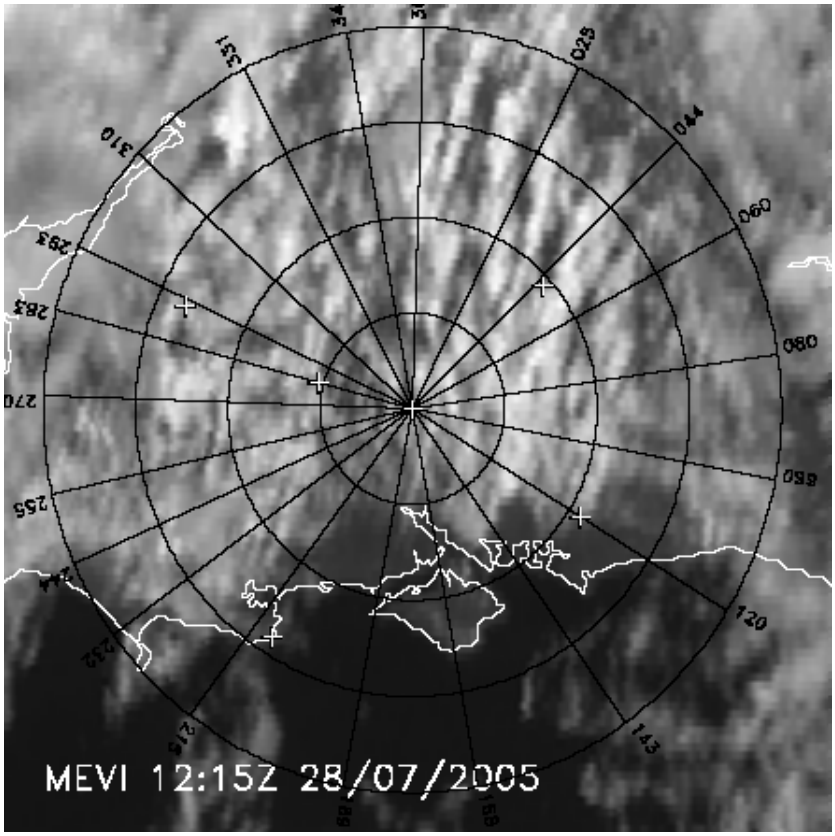

(b)

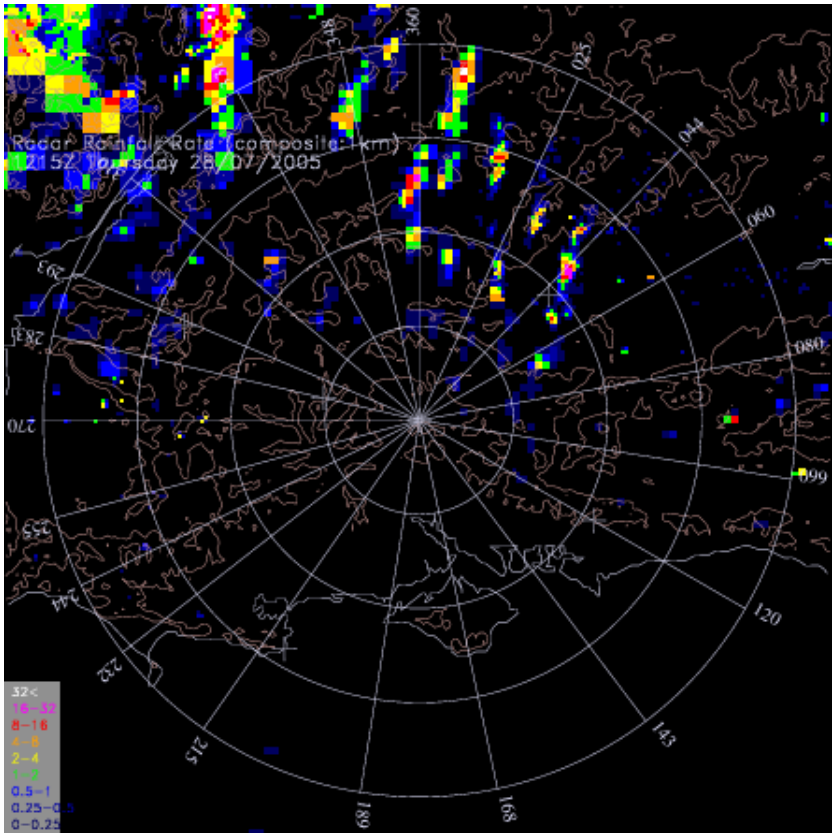

Figure 12: (a) High-resolution visible image from Meteosat-8 (MSG) and (b) rainfall rate from the radar network (key in mm h^{-1}) at 1215 UTC on 28 July 2005 (IOP 12), showing convective cloud streets and associated thunderstorms. Range rings are centered on Chilbolton and plotted every 25 km.

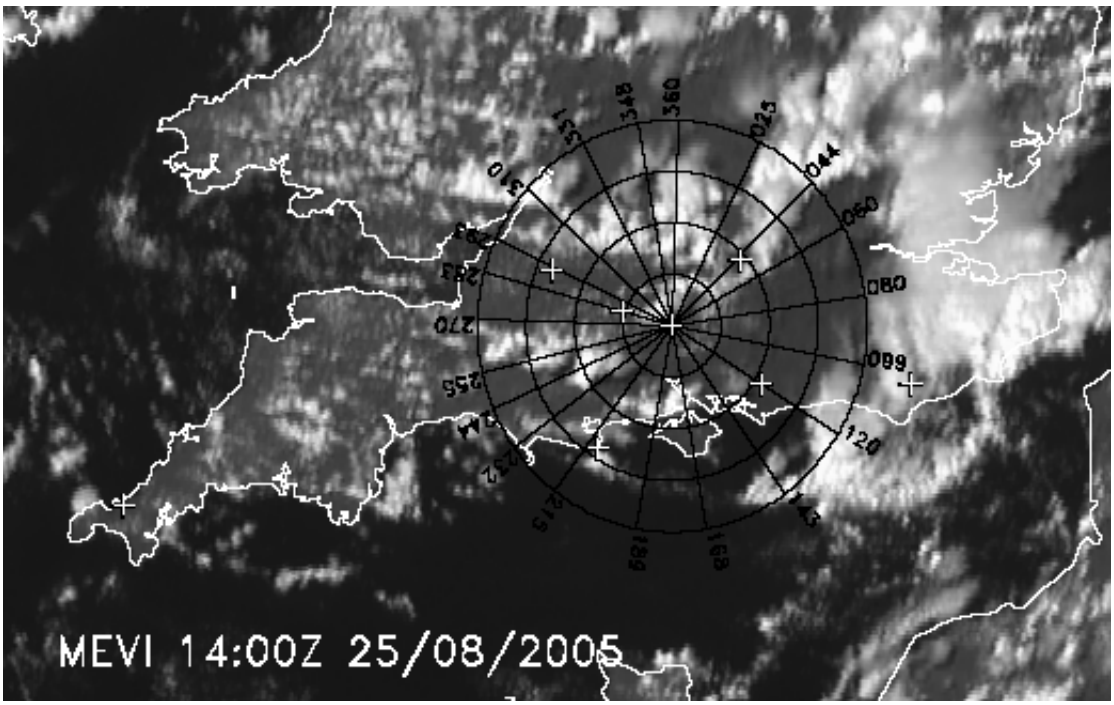

Figure 13: Similar to Fig. 10, but for 1400 UTC on 25 August 2005 (IOP 18), showing an arc of convective cloud along a gust front to the SE of Chilbolton over the English Channel.

(a)

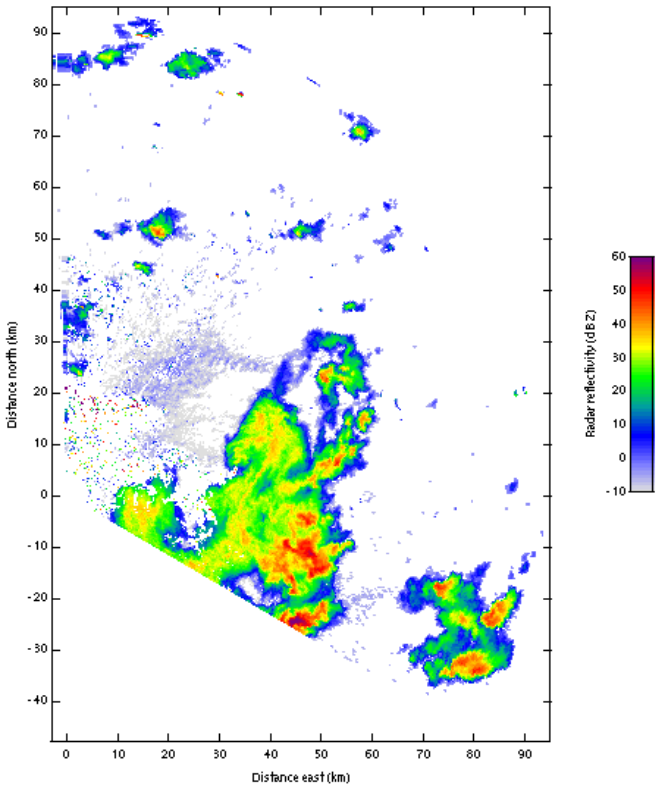

(b)

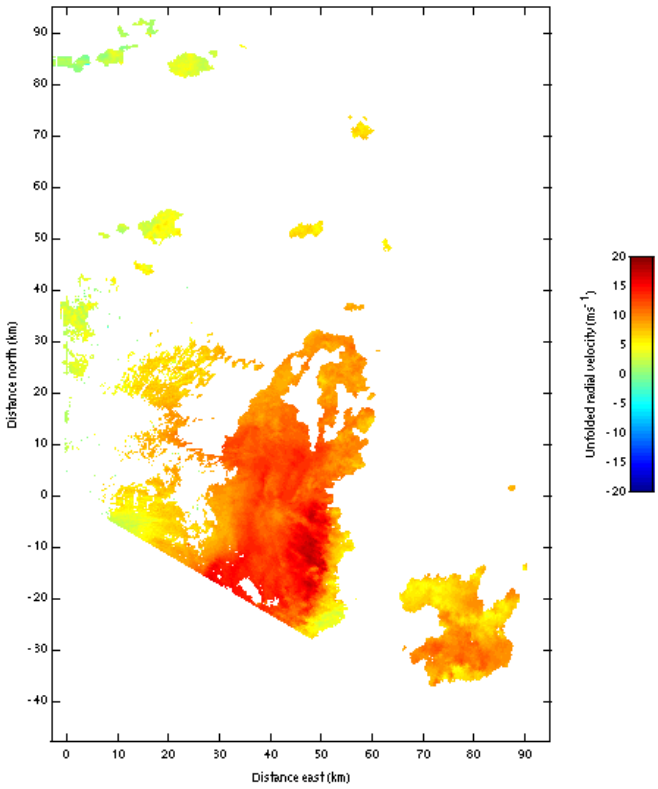

Figure 14: Example of a cold-pool-outflow convergence line: PPIs at 0.5 deg of (a) reflectivity (dBZ) and (b) unfolded Doppler velocity (m s^{-1} away from radar) at 1157 UTC on 25 August 2005 (IOP 18) showing the relation between convergence features and the precipitation field.

(a)

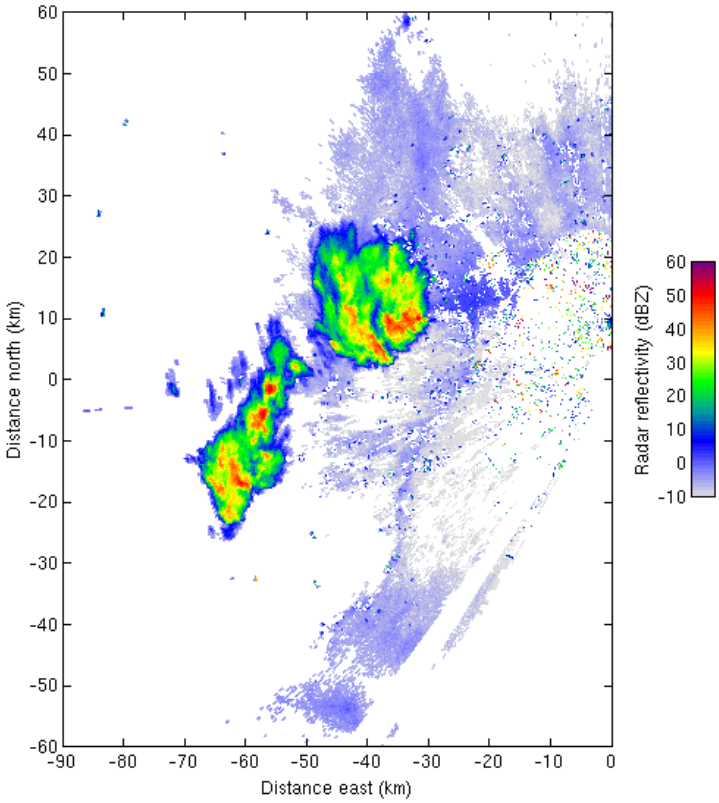

(b)

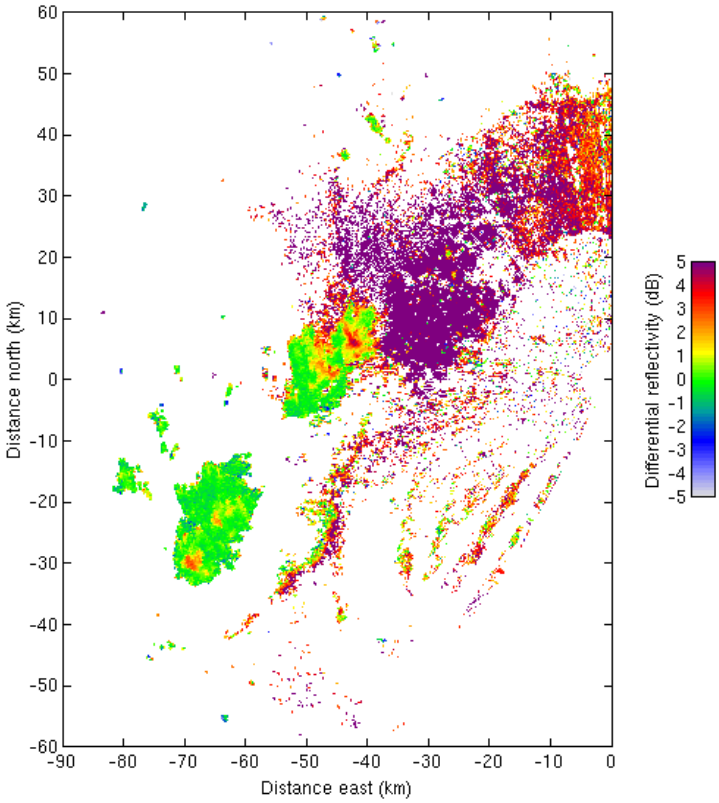

Figure 15: PPIs at 0.5 deg of (a) reflectivity (dBZ) at 1701 UTC and (b) differential reflectivity (dB) at 1622 UTC on 18 August 2005 (IOP 16), showing a radar fine line associated with a gust front.

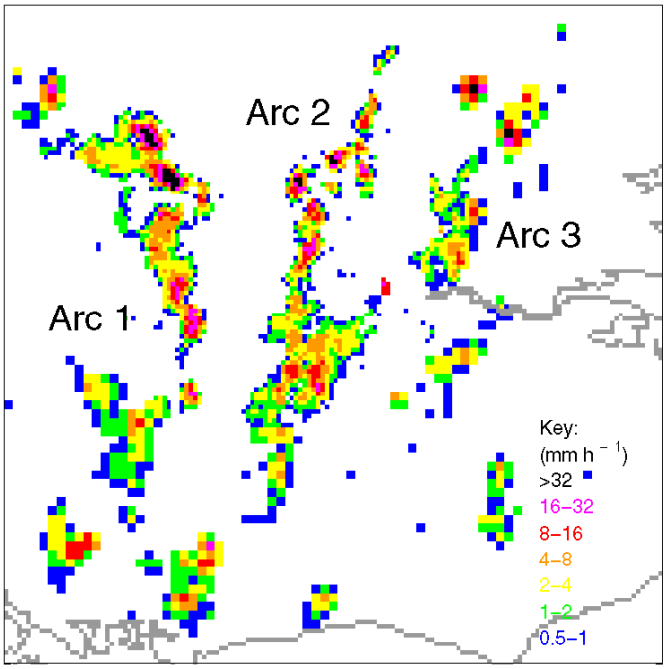

Figure 16: Rainfall rate (mm h^{-1}) over a 150 km x 150 km region of southern England at 1130 UTC on 10 July 2004, showing a series of precipitation bands that had been triggered by a gravity wave generated by an earlier storm. (From Morcrette et al. 2006).

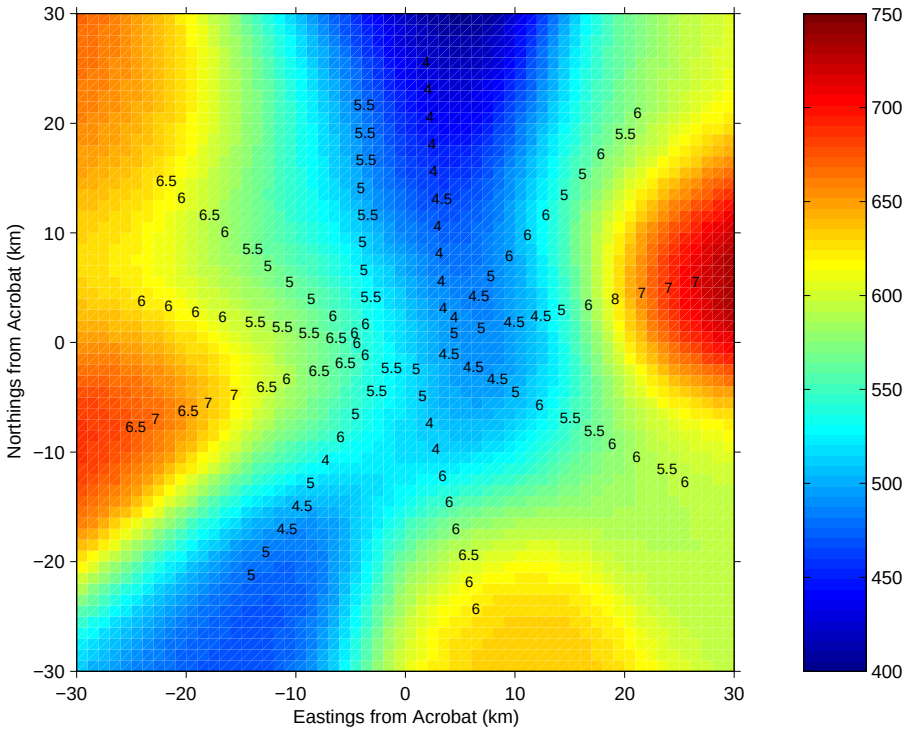

Figure 17: Height of boundary-layer top (hundreds of meters), with interpolated heights shown in color (according to the key, in meters) as derived from ten RHI scans with the 1275 MHz Chilbolton radar. The variation in height is believed to be due to the gravity wave that triggered the precipitation bands in Fig. 16. The scans were obtained from 0751 to 0807 UTC and their positions have been displaced to correspond to 0758 UTC assuming a system velocity of 8 m s^{-1} from the west. (From Morcrette et al. 2006).

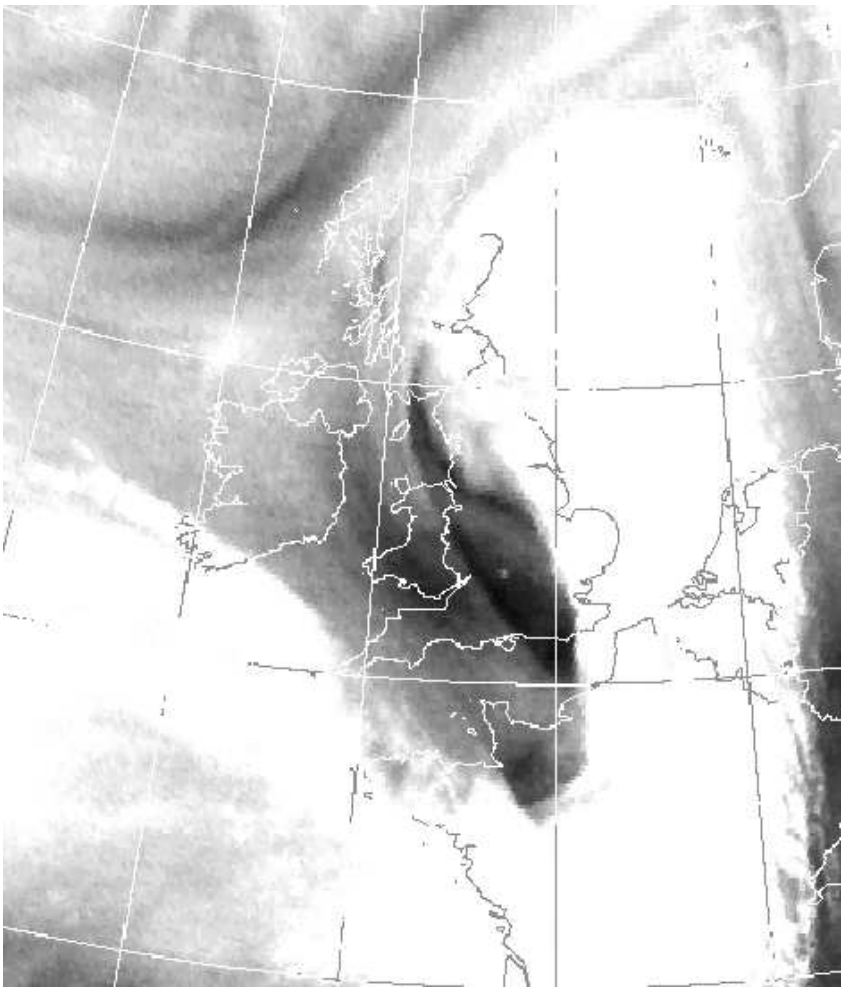

Figure 18: Rapid-scan Meteosat water-vapor image at 1200 UTC on 15 June 2005 (IOP 1), showing a thunderstorm (very small gray dot) within a water vapor dark zone. The image is enhanced to clarify the position of this thunderstorm with respect to the dark zone; although the surrounding white areas are saturated, there is no information in these areas relevant to the discussion. Because the thunderstorm was shallow, it does not show up as a major feature in the water vapor imagery which is sensitive mainly to features in the upper troposphere.

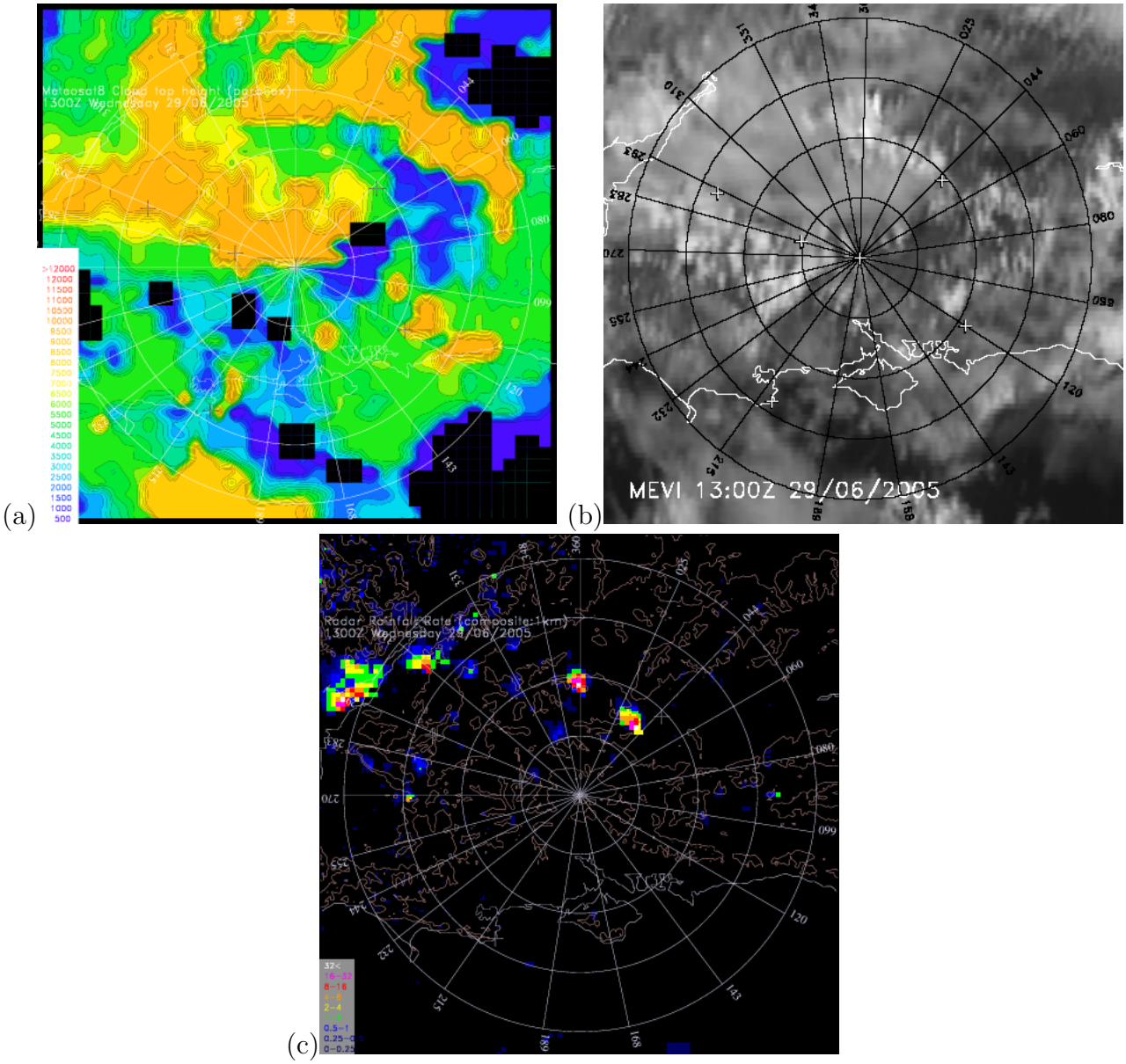

Figure 19: (a) Cloud-top height (m) derived from MSG infra-red data, (b) MSG high-resolution visible image and (c) radar-network rainfall rate, at 1300 UTC on 29 June 2005 (IOP 5), showing the possible effect of shadowing by cirrus anvils on the formation of new convective clouds. Range rings are centered on Chilbolton and plotted every 25 km.

(a) (b)

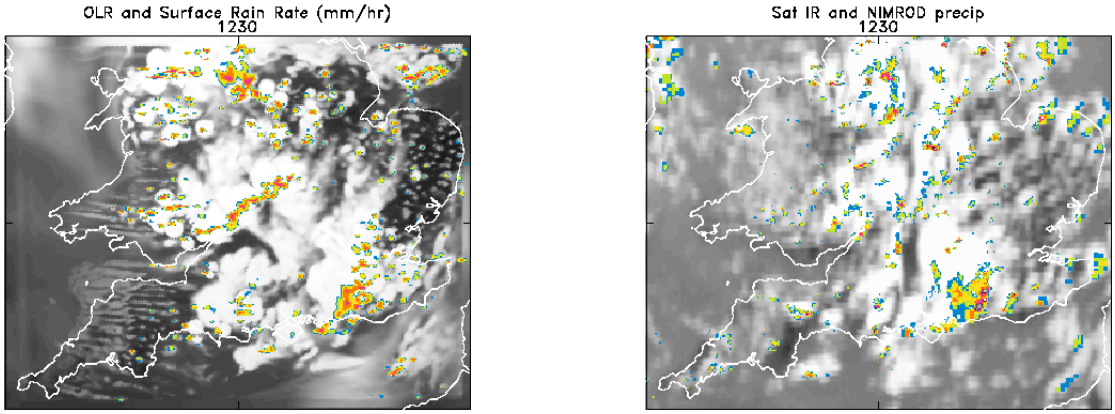

Figure 20: (a) Unified Model 6.5-hour forecast of broadband IR radiance temperature and surface rainfall rate compared with (b) observational analysis showing NIMROD-derived rainfall rate (colors) superimposed on IR satellite-derived cloud (white), at 1230 UTC on 25 August 2005 (IOP 18).